Origin of the stabilized simple-cubic structure in polonium: Spin-orbit interaction versus Peierls instability

B. I. Min,[1] J. H. Shim,[1] Min Sik Park,[1] Kyoo Kim,[1] S. K. Kwon,[1,*] and S. J. Youn[2]
[1]*Department of Physics, Pohang University of Science and Technology, Pohang 790-784, Korea*
[2]*Department of Physics Education, Gyeongsang National University, Jinju 660-701, Korea*
(Received 8 March 2006; published 7 April 2006)

The origin of the stabilized simple-cubic (SC) structure in Po is explored by using the first-principles band calculations. We have found that the prime origin is the inherent strong spin-orbit (SO) interaction in Po, which suppresses the Peierls-type structural instability, as usually occurs in *p*-bonded systems. Based on the systematic analysis of electronic structures, charge densities, Fermi surfaces, and susceptibilities of Se, Te, and Po, we have proven that the stable crystal structure in VIA elements is determined by the competition between the SO splitting and the crystal-field splitting induced by the low-symmetry structural transition. Our study suggests that the large SO interaction would suppress the Peierls instability which is generally expected to occur in one-dimensional conductors.

DOI: 10.1103/PhysRevB.73.132102 PACS number(s): 61.66.Bi, 71.70.Ej, 71.20.Gj

Among the elements in the periodic table, only Po (polonium) is known to crystallize in the simple-cubic (SC) structure in nature.[1] Radioactive Po, which was discovered by Pierre and Marie Curie in 1898, requires difficult sample preparation, and so not many experimental and theoretical studies have been carried out. Po, which is located in the VIA column of the periodic table, has a valence electron configuration of $6s^2 6p^4$ ($Z=84$), and exhibits two metallic phases of α and β which are formed in the SC and the rhombohedral (trigonal) structure below and above ~ 348 *K*, respectively.[2,3] Note that the isoelectronic elements located in the same VIA column, Se (selenium) and Te (tellurium), crystallize in the trigonal structure (space group $P3_121$) with the helical chain arrangements of atoms, which run parallel to the crystallographic *c* axis of the hexagonal setting [see Fig. 1(a)].[4] Hence, the coordination number is 2 in trigonal Se and Te in contrast to 6 in simple-cubic Po (SC-Po). The ratio of the intrachain (d_1) bond length to the interchain (d_2) bond length is $d_2/d_1=1.50$, 1.23, and 1.0 for Se, Te, and Po, respectively. The coordination number of 2 in trigonal Se and Te can be understood based on the simple octet rule.[5]

The reason why metallic Po has a stable SC structure has been addressed in the literature, but questions still remain. By using the relativistic parameterized extended Hückel method, Lohr[6] found a hint that the helical structure as a distortion of a SC structure might be quenched in the case of Po due to its very large spin-orbit (SO) coupling. However, the calculation in Ref. 6 was not self-consistent and the atomic value of the SO coupling parameter was adopted. The structural energetics was also not studied in Ref. 6. Recently, using the pseudopotential band method, Kraig *et al.*[7] showed that the SC structure is preferred by Po to face-centered-or body-centered-cubic structure. They argued that the large *s*-*p* splitting in Po would produce the stable SC structure. However, they could not explain why this happens only in Po, but not in other elements with similarlylarge *s*-*p* splittings. Moreover, neither the internal atomic distortion nor the SO interaction was taken into account in their band calculations. Lach-hab *et al.*[8] studied the structural energetics for Po using the tight-binding (TB) band method. After having determined the TB parameters by fitting the TB bands to the semirelativistic full-potential linearized augmented plane-wave (FLAPW) bands,[9] they took account of the SO effect *a posteriori* by employing the atomic value of the SO coupling parameter. They found that the SC structure is the most stable among the close-packed structures for both cases with and without the SO effect included. They did not consider the lower symmetry structures with the internal atomic relaxation, as observed in Se and Te.

A systematic crystallographic transformation can occur from the SC lattice to the trigonal lattice. As shown in Fig. 1(b), the SC lattice can be described by a hexagonal lattice in which the hexagonal *a* axis corresponds to the face diagonal and the hexagonal *c* axis to the body diagonal of cube. Then, the size of the unit cell becomes tripled with $c/a=\sqrt{3/2}$. The trigonal structure of β-Po corresponds to theelongated SC structure simply along the body diagonal direction. In the trigonal structures of Se and Te, the internal atomic position parameters are also changed, in addition to elongation.[10]

To explore the origin of stabilized SC structure in Po, we have investigated the electronic and structural properties of Se, Te, and Po systematically by using the first-principles

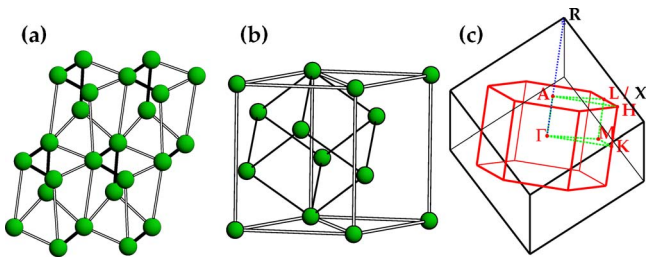

FIG. 1. (Color online) (a) Crystal structure of Se which can be formed from the SC structure via internal atomic distortions. The helical chain arrangements of Se atoms are denoted by thick solid lines. (b) A hexagonal unit cell with tripled volume of a SC unit cell. (c) The hexagonal Brillouin zone (BZ) compared to the SC BZ. Note that Γ-A and Γ-L in the hexagonal BZ correspond to $\frac{1}{3}$Γ-R and Γ-X in the SC BZ.

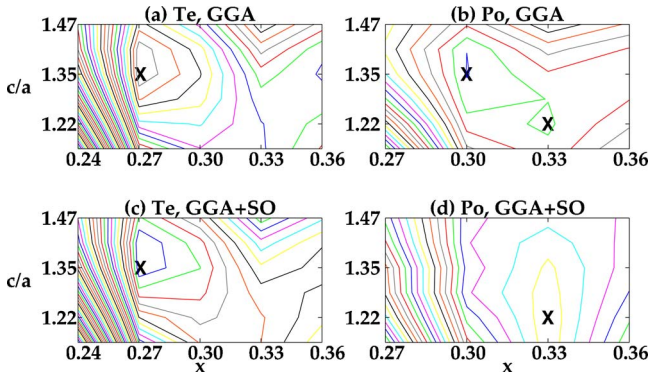

FIG. 2. (Color online) Total energy contour plots for Te and Po as functions of the internal atomic parameter x and c/a. X mark denotes the total energy minimum position. Both in the GGA (a) and GGA+SO (c), Te shows a global minimum at the trigonal (T) structure. In the GGA (b), Po shows two minima, one global at T and one local at SC. Note that the SC structure corresponds to the point of $x=1/3$ and $c/a=\sqrt{3/2}\approx 1.22$. In the GGA+SO (d), Po shows only one global minimum at SC.

FLAPW band method incorporating the SO interaction. For the calculations, the QMD-FLAPW (Ref. 9) and the WIEN2K (Ref. 11) codes are utilized. The band structure results obtained from both codes are qualitatively coincident with each other. Below, we will use mainly WIEN2K results, since the local orbital basis is implemented in WIEN2K in order to describe the relativistic $6p_{1/2}$ wave function correctly.[12] The exchange-correlation interaction is treated by the generalized gradient approximation (GGA).[13,14]

We have first studied the structural energetics by optimizing the atomic positions for both trigonal and SC structures of Se, Te, and Po with and without the SO interaction included.[15] Let us call the former the GGA,and the latter the GGA+SO scheme. In the GGA scheme, the trigonal structures are more stable than SC structures by 0.092, 0.031, and 0.004 eV/atom for Se, Te, and Po, respectively. The GGA +SO scheme, however, yields different results. The incorporation of the SO coupling reduces the stability of the trigonal structure. For Se and Te, the trigonal structure is still more stable than the SC structure by 0.090 and 0.021 eV/atom, respectively. In contrast, for Po, the SC structure becomes more stable than the trigonal structure by 0.016 eV/atom. The calculated equilibrium volume of SC-Po is 37.15 Å, which is in good agreement with the observed 37.60 Å.[16] This feature is clearly seen in Fig. 2, which provides the total energy contour plots in the structural space. In the GGA for Te, there is a global minimum at the trigonal (T) structure, whereas, for Po, there are two minima, one global at T and one localat SC. The SO coupling does not affect the global minima in Se and Te, but changes that in Po from trigonal Po to SC-Po. This finding indicates that the SO interaction plays an essential role in stabilizing the SC structure of Po.

Indeed, band structures in Figs. 3(a) and 3(b) reveal that the effect of the SO interaction is substantial for SC-Po, as compared to that for Se and Te. The lowest bands in Figs. 3(a) and 3(b) correspond to Po $6s$ states, while the bands near the Fermi level (E_F) correspond to Po $6p$ states. Due to the large energy gap between the $6s$ and $6p$ states, there will

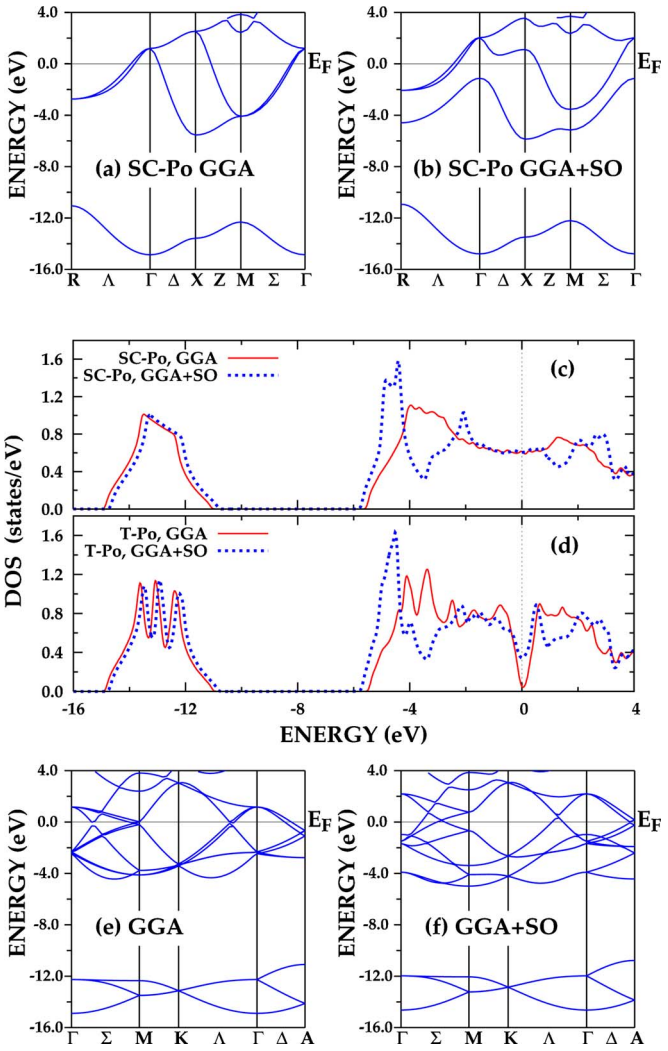

FIG. 3. (Color online) (a) and (b) The GGA and GGA+SO band structures of SC-Po. (c) and (d) DOSs of SC-Po and trigonal Po. The latter corresponds to the stable phase obtained after the structural optimization in the GGA scheme. In each frame, DOSs obtained by the GGA and GGA+SO schemes are compared. (e) and (f) The GGA and GGA+SO band structures of SC-Po drawn in the frame of the hexagonal BZ. There are several band crossings at E_F in the GGA, but not in the GGA+SO.

not be a considerable mixing between them, and thus Po can be classified as a p-bonded system. When the SO interaction is taken into account, the degenerate $6p$ bands along Γ-X, Γ-M, and Γ-R are split so that the doubly degenerate $6p_{1/2}$ band is separated from the upper half-filled $6p_{3/2}$ band. Due to the SO splitting, the small hole Fermi surface at Γ disappears. The SO splitting of p states at Γ for SC-Po is as much as 3.16 eV, which is much larger than those for SC structures of Se and Te, 0.53 and 1.05 eV.

In Figs. 3(c) and 3(d), we have compared the density of states (DOS) of SC-Po and that of trigonal Po, which are obtained by the GGA and GGA+SO schemes. Here, trigonal Po corresponds to the stable phase determined by the structural optimization in the GGA scheme. In Fig. 3(c), one can see clearly the splitting of bands at around −3.5 eV due to the SO interaction. Notable in the GGA−DOS is the

pseudogap feature at E_F for trigonal Po, which would give rise to the semimetallic behavior. The pseudogap appears between the nonbonding lone pair and the antibonding Po $6p$ state, because of the splitting between the bonding and antibonding Po $6p$ state in the chain arrangement of trigonal Po.[4] Hence, the DOS at E_F, $N(E_F)$, becomes greatly reduced in trigonal Po from that in SC-Po. In fact, the stable trigonal phases of Se and Te result from this gap formation near E_F. In the case of Se, the energy splitting between the bonding and the antibonding state is so large that the system becomes insulating, while Te is semimetallic.

In the GGA+SO scheme, the $6p_{1/2}$ state is separated out, and so the band shape and N(E_F) are changed a lot. Occupied band widths are broadened with more weight at the low-energy side, which produces energy gains for both SC-Po and trigonal Po. The stable SC-Po in the GGA+SO scheme reflects that the SO induced energy gain is larger for SC-Po than for trigonal Po. It is because $N(E_F)$ for trigonal Po is rather enhanced producing some energy loss. Note that, for Se and Te, both the GGA and GGA+SO schemes yield similar DOS, implying no noticeable energy gain from the SO interaction.[16] These results suggest that the stable crystal structure in VIA elements is mainly determined by the competition between the SO splitting and the crystal-field splitting due to the low-symmetry structure. That is, for Se and Te, the larger crystal-field splitting between the intrachain bonding and antibonding states stabilizes the trigonal structure, whereas, for Po, the larger SO splitting stabilizes the SC structure.

The stable trigonal structure of Se and Te can be understood in terms of the three dimensional (3D) Peierls distortion of the SC structure.[5,10,17] In general, p-bonded systems would favor the SC structure to maximize the directional p_σ bonding. However, three mutually orthogonal linear chains in the SC structure will be easily distorted by the Peierls mechanism when the linear chain is partially filled. In the case of Se and Te, each chain is two-thirds filled, andso the energy gain can be achieved by the trimerization with the short-long-long bond alternation. Decker *et al.*[18] recently demonstrated this mechanism for Te by comparing the band structures of the undistorted SC and the distorted trigonal structure. The structural distortion from the SC to the trigonal structure induces a splitting of degenerate bands near E_F, which yields the energy gain for trigonal Te.

We have examined the above scenario for SC-Po. Figures 3(e) and 3(f) display the GGA and GGA+SO band structures of undistorted SC-Po which are projected in the hexagonal BZ. The GGA band of Fig. 3(e) shows several band crossings at E_F which are created by the backfolding of bands of the larger SC BZ into the smaller hexagonal BZ [see Fig. 1(c)]. Then, as in Te,[18] a Peierls-type structural distortion would split the band crossings at E_F to yield the energy gain. In contrast, the GGA+SO band of Fig. 3(f) shows the band crossings not at E_F but at higher- or lower-energy side far apart from E_F. This is because of the substantial band shift by the SO splitting. Accordingly, no energy gain would result from the Peierls-type structural distortion. This proves how the SO interaction stabilizes the SC structure of Po. When Decker *et al.*[18] demonstrated this mechanism for Te, they did not take into account the SO interaction. The SO-induced band shift in Te, however, is not large enough to suppress the Peierls-type instability. This demonstration reveals that the large SO interaction would suppress the Peierls instability which is generally expected to occur in one-dimensional (1D) conductors.

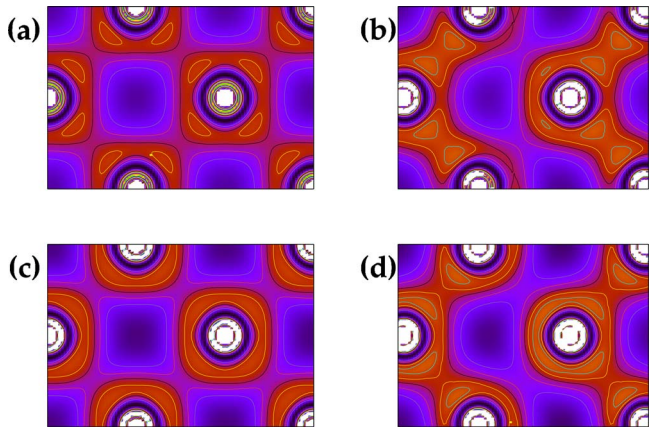

FIG. 4. (Color online) The occupied charge density distributions of Po $6p$ bonding states in the energy range of −6.0−−3.0 eV. (a) SC-Po (GGA), (b) trigonal Po (GGA), (c) SC-Po (GGA+SO), and (d) trigonal Po (GGA+SO).

The bonding characters can be investigated by the charge density plot. Figure 4 shows the occupied charge density distributions of Po $6p$ bonding states in the energy range of −6.0−−3.0 eV for both SC-Po and trigonal Po. They are plotted on the special plane of the hexagonal unit cell to see the bonding character along the helical zig-zag chains in the c direction. The GGA charge density for SC-Po [Fig. 4(a)] shows larger bonding character between Po atoms than the GGA+SO charge density [Fig. 4(c)]. This implies that the directional bonding between atoms becomes weakened when incorporating the SO interaction, and so the charge density becomes more isotropic. This feature is more clearly seen in trigonal Po which manifests the prominent chain nature. The GGA charge density for trigonal Po [Fig. 4(b)] shows a pronounced intrachain bonding character along the zig-zag chains. In the GGA+SO charge density [Fig. 4(d)], the SO interaction weakens the intrachain directional bondings so that the anisotropic chain nature is suppressed. This is consistent with the enhanced $N(E_F)$ in the GGA+SO DOS in Fig. 3(d). The charge density plots reveal that the SO interaction weakens the directional bondings between Po atoms, and so suppresses the 1D chain nature and the corresponding Peierls-type structural instability.

The structural transition can also be studied by analyzing the behavior of the charge susceptibility $\chi_0(q)$. $\chi_0(q)$'s in Fig. 5(c) are obtained from the band structures of SC-Po. $\chi_0(q)$ in the GGA scheme shows the highest peak near $\vec{Q}=2/3\Gamma$-R, indicating a possible structural instability at this $\vec{Q}$. This $\vec{Q}$ vector is coincident with the reciprocal lattice vector connecting the hexagonal BZ boundaries including A [see Fig. 1(c)], at which the bands of SC-Po along Γ-R are folded back. Therefore, this peak is closely related to the trigonal distortion of the SC structure along the (111) direction. Noteworthy in Fig. 5(c) is the substantial reduction of

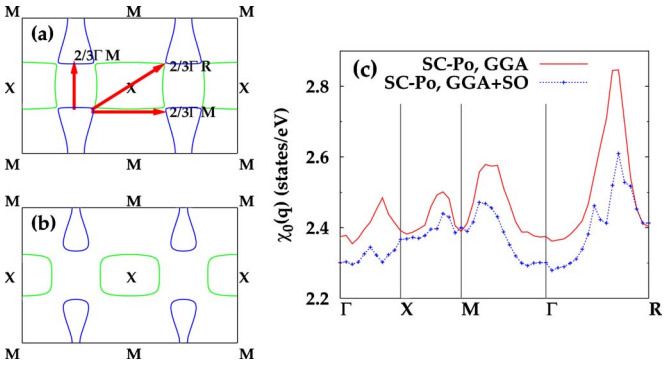

FIG. 5. (Color online) Fermi surfaces of SC-Po derived from the third (green) and fourth (blue) bands in the GGA (a) and the GGA+SO (b). (c) Susceptibilities $\chi_0(q)$ of SC-Po in the GGA and the GGA+SO. Arrows in (a) denote the nesting vectors producing peaks in $\chi_0(q)$.

this peak of $\chi_0(q)$ when incorporating the SO interaction. The absence of the structural instability in Po would be closely correlated to this behavior of $\chi_0(q)$. One can also note the peaks in $\chi_0(q)$ near $\vec{q}$=2/3Γ-X, 2/3Γ-M, 2/3X-M. These peaks and the peak near $\vec{Q}$ are expected to arise from the quasi-1D Fermi surfaces of SC-Po, which are formed by the third and fourth bands in Fig. 3(a). Namely, each $\vec{q}$ producing the peak in $\chi_0(q)$ corresponds to the nesting vector of the quasi-1D Fermi surfaces projected in each symmetry plane. The GGA Fermi surfaces in Fig. 5(a), which are drawn in the (220) plane of the SC BZ, exhibit the clear quasi-1D nature with the corresponding nesting vectors. As shown in Fig. 5(b), the SO interaction breaks these quasi-1D Fermi surfaces into pieces, and so reduces the nesting effect. This situation in Po is different from that in Se and Te, in which the 1D nature is preserved even with the SO interaction, so that the nesting effect is still active.

Finally, it is worthwhile to discuss the stable structures of neighboring elements of Po, Bi (Z=83) and At (Z=85), both of which are also p-bonded metallic systems with the large SO interaction. In nature, Bi crystallizes in the trigonal (α-arsenic) structure.[19] The α-arsenic structure of Bi can be understood as arising from the Peierls-type distortion, as discussed above.[5,17] Since the 6p bands in Bi are half-filled, the tendency of the Peierls instability is predominating so as to drive the structural distortion despite the large SO interaction. As for radioactive At, no structural information is available because of its too short half-life of only 8.3 h. The 6p bands of At are 5/6-filled so that the SO interaction would dominate over the Peierls instability as in Po. Hence, the SC structure is expected to be stabilized for At.

In conclusion, we have clarified that the origin of the stabilized SC structure in Po is its inherent strong SO interaction. The large SO interaction in Po weakens the directional bondings between atoms so as to suppress the Peierls-type distortion. Further, the stable crystal structure in VIA elements is determined by the competition between the SO splitting and the crystal-field splitting induced by the Peierls-type structural transition to a lower symmetry. Our study also reveals that the large SO interaction would suppress the Peierls instability which is generally expected to occur in 1D conductors.

This work was supported by the SRC program of MOST/KOSEF.

*Present address: Dept of Chemistry, POSTECH, Pohang 790-784, Korea.

[1] W. H. Beamer and C. R. Maxwell, J. Chem. Phys. **14**, 569 (1946).
[2] C. R. Maxwell, J. Chem. Phys. **17**, 1288 (1949).
[3] R. J. Desando and R. C. Lange, J. Inorg. Nucl. Chem. **28**, 1837 (1966).
[4] J. D. Joannopoulos, M. Schlüter, and M. L. Cohen, Phys. Rev. B **11**, 2186 (1975).
[5] J.-P. Gaspard, A. Pellegatti, F. Marinelli, and C. Bichara, Philos. Mag. B **77**, 727 (1998).
[6] L. L. Lohr, Inorg. Chem. **26**, 2005 (1987).
[7] R. E. Kraig, D. Roundy, and M. L. Cohen, Solid State Commun. **129**, 411 (2004).
[8] M. Lach-hab, B. Akdim, D. A. Papaconstantopoulos, M. J. Mehl, and N. Bernstein, Solid State Commun. **65**, 1837 (2004).
[9] E. Wimmer, H. Krakauer, M. Weinert, and A. J. Freeman, Phys. Rev. B **24**, 864 (1981); M. Weinert, E. Wimmer, and A. J. Freeman, *ibid.* **26**, 4571 (1982); H. J. F. Jansen and A. J. Freeman, *ibid.* **30**, 561 (1984).
[10] G. Kresse, J. Furthmuller, and J. Hafner, Phys. Rev. B **50**, 13181 (1994).
[11] P. Blaha, K. Schwarz, G. K. H. Madsen, K. Kvasnicka, and J. Luitz, WIEN2K (Karlheinz Schwarz, Technische Universitat Wien, Austria, 2001).
[12] D. Singh, *Plane waves, Pseudopotentials, and the LAPW Method* (Kluwer Academic, Boston, 1994).
[13] J. P. Perdew, K. Burke, and M. Ernzerhof, Phys. Rev. Lett. **77**, 3865 (1996).
[14] We have found that the GGA describes the ground states of Se, Te, and Po better than the LDA.
[15] After checking the convergence test, we have obtained the ground state properties of Po, such as band structure and DOS in Fig. 3 and the charge density in Fig. 4, using APW plane waves with $R_{\mathrm{MT}}\vec{K}_{\mathrm{max}}$=9 and 8000$\vec{k}$ points in the full BZ. For structural optimization and energetics for Se, Te, and Po, as shown in Fig. 2, we have used $R_{\mathrm{MT}}\vec{K}_{\mathrm{max}}$=9 and 847$\vec{k}$ points in the full BZ. Employed muffin-tin radii R_{MT} for Po, Te, and Se are 2.5, 2.4, and 2.2 a.u., respectively.
[16] J. H. Shim, M. S. Park, and B. I. Min (unpublished).
[17] J. K. Burdett and S. Lee, J. Am. Chem. Soc. **105**, 1079 (1983).
[18] A. Decker, G. A. Landrum, and R. Dronskowski, Z. Anorg. Allg. Chem. **628**, 295 (2002).
[19] A. B. Shick, J. B. Ketterson, D. L. Novikov, and A. J. Freeman, Phys. Rev. B **60**, 15484 (1999).